Applications of Terrestrial Laser Scanning for deformation analyses of an adaptive supporting structure

S. I. Poptean, A. F. Jocea
Department of Surveying and Cadastre, Faculty of Geodesy, Technical University of Civil Engineering of Bucharest, Lacul Tei Blvd., no. 122-124, sector 2, 020396, Bucharest, Romania

A. Schmitt, V. Schwieger
Institute of Engineering Geodesy, University of Stuttgart, Geschwister-Scholl-Straße 24 D, 70174, Stuttgart, Germany

M. Heidingsfeld, O. Sawodny
Institute for System Dynamics, University of Stuttgart, Waldburgstraße 17/19, 70563, Stuttgart, Germany

Abstract. Structural deformation represents a serious reaction parameter regularly measured for structural health monitoring. For a better understanding of structural behavior, the measurements of the deformations of a supporting structure using the capabilities of a terrestrial 3D laser scanner were realized. The adaptive supporting structure Stuttgart SmartShell can be shifted in three directions by given amounts at three different joints. The surface deformations originated by these shifts were simulated using the Finite Element Method (FEM). A Leica HDS7000 Laser Scanner was used to acquire a point cloud representing the deformed structure as a whole. Shifts were performed at the three joints in different directions. The measured surfaces were compared to each other and to the simulated deformations. The significance of these differences was statistically tested. Simulations and measurements show almost no significant differences.

Keywords. Structural deformations, FEM, behavior, terrestrial laser scanning

1 Introduction

One of the most complex tasks in the field of geodetic surveying is considered to be monitoring of the displacements and deformations of natural and artificial structures and objects.
Monitoring objects and structures behavior is an activity which could take place throughout the life of the object starting from the construction. It consists of a systematic process of gathering and use of the information achieved through the observation or measurements of phenomena that describe the objects and structures sizes and properties in the interaction process with the natural and technological environments.
The main objective of objects and structural monitoring is to determine certain parameters such as foundation soil, groundwater level and wind action or temperature change that describe and explain the behavior of objects or rather structures. These static or dynamic factors result from the measurements made by applying different geodetic methods and technologies. Inter alia Eling (2009) and Zoog and Ingensand (2008) show that laser scanning is a useful technology for geodetic monitoring.
In this paper a study of deformation applied to a thin shell structure will be presented at different measurement epochs. The aim is to verify the simulation model and compare it with the reality. This purpose is realized, taking into account that the loads are simulated by shifting the structure's supports.
The main subject matter is the monitoring of deformations arising from implementation of controlled structural displacements and the comparison of obtained results with simulation results that are based on an idealized mathematical model.
Nowadays objects or rather structures are designed for a specific maximum load, that only occurs rarely and for a short period of time. Therefore much of the heavy, costly material used today only occasionally proves to be necessary (Neuhäuser et al, 2012). In this case, an ultra-lightweight structure that reduces the use of material in comparison to conventional passive structures by actively adapting to varying loads is recommended.

2 Finite Element Model of the Structure

2.1 Background the Finite Element Method

The Finite Element Method (FEM) is a numerical method to approximately solve partial differential equations that commonly result from physical problems in various engineering domains. Due to its versatility and efficiency, the FEM is the de facto standard for stress and deformation analysis in structural mechanics (Bathe, 2002). The general procedure is to first divide a complex structure into small elements. Within each element, a linear combination of shape functions is then used to describe the general solution to the problem as a function of yet unknown parameters. Evaluation of the shape functions at the element boundaries, the so-called nodes, results in a linear system of equations for the unknown parameters, which can be solved numerically. In practice, commercially available software tools are used to perform these steps.

2.2 Presentation of the Stuttgart Smart Shell

The Stuttgart SmartShell (Fig. 1) is an open-air shell structure that has a base area of around 100 square meters and a thickness of only 4 centimeters, which is about one third the thickness of a conventional civil structure of comparable shape and size. It is made of a multi-layer wood laminate, with the fibers of each of the four layers arranged perpendicularly.

Fig 1 Stuttgart SmartShell © Bosch Rexroth, 2012

The doubly-curved timber body is resting on four points, one of which is a static support while the other three are mobile supports. That mobile support can be moved individually using three hydraulic drives arranged in a tripod configuration at each support (Fig. 2).

Fig 2 Hydraulic drives

Strain gauges registering the local deformation are installed in various locations underneath the shell (Fig. 3). These sensors are linked to a control system responsible for the support displacements of the shell structure. When a change in the structural load is detected – due to snowfall or wind – the system is able to react by producing certain support displacements to compensate for the stress in the material caused by the external loads. During this investigation the data of the strain gauges are not considered because Neuhäuser (2014) showed already large differences between the measurements and the results from simulations and he could not find any reason for these discrepancies.

Fig 3 Load registration sensors

To determine the support displacements necessary to compensate for the external loads, optimization algorithm based on computer simulation models of the structure were developed. These models predict the behavior of the structure under external loads, thus being able to precisely calculate the required counter-movements. Additionally, active damping of structural vibrations is implemented (Neuhäuser et al., 2012).

In conclusion, the main purpose of this type of construction is to use active manipulation of the structure in order to reduce structural stress and vibrations, at the same time acquiring a drastic weight reduction.

2.3 Resulting Models

The finite element model of the Stuttgart SmartShell was generated with the software package ANSYS. The structure is divided in 3134 elements of SHELL181 type. It has 3349 nodes with three translational and three rotatory degrees of freedom at each node. The model permits to calculate the deformation of the structure for any given support displacement. To increase the accuracy of the calculations, the methods of non-linear finite element analysis are used (Neuhäuser et al, 2012).

3 Measurement and processing of Terrestrial Laser Scans

3.1 Measurement setup and Data Acquisition

Data acquisition was proceeded using Leica HDS 7000 and involved the controlled displacement of three out of four supports of a thin shell structure SmartShell in an outdoor test frame based in Campus Vaihingen at University of Stuttgart. The displacements were applied by a hydraulic system which moves the three mobile supports in the directions of the three axes, X, Y and Z (Fig. 4).

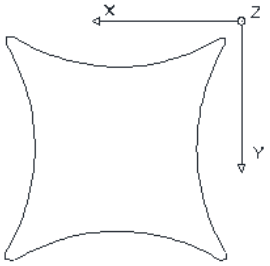

Fig 4 The 3-axis directions relative to the structure

The supports were moved 20 mm one at a time in each of the three directions and after each move the structure was brought back to the initial position. A total of 9 displacements were applied (Fig. 5). The initial position was measured in the beginning, this way allowing the capturing of a zero-displacement case. In the end, a total of 10 measurement epochs were acquired.

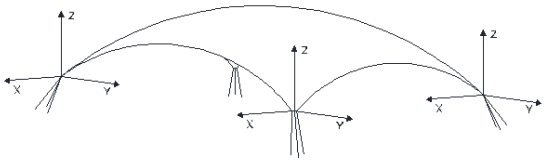

Fig 5 Applied displacements of the structure

For data acquisition, the laser scanner was positioned approximately in the middle of the measured structure (Fig. 6), in order to achieve balanced data densities for the whole measured surface and to minimise the probability of small angles of incidence of the laser beam on the surface. However, the erroneous angles of incidence could not be fully avoided due to the existence of load sensor boxes on the surface of the shell, which were not correctly registered by the laser scanner. The measurements were conducted on dry weather, at approximately 4^0C and 50% air humidity.

Fig 6 HDS 7000 laser scanner position

For each measuring epoch, the scanning was performed at high resolution, capturing 10000 pixels per 360^0 horizontally and vertically, and normal quality, meaning that every scan took 3:22 minutes. The entire inner surface of the shell structure was scanned 10 times, in the beginning and after each displacement configuration. For each measured point, two angles, a distance and the reflection intensity were recorded, which were transformed into Cartesian coordinates, resulting in a point cloud with X, Y, Z coordinates and an intensity value for each point.

3.2 Data Processing

The second phase of the study was data processing. Due to the fact that laser scanners are gathering all the details that appear in the field of view and because not all collected data is significant, the area-wise deformation analysis required a filtering of the 3D data. This operation was done manually using Leica Cyclone software (Fig. 7). For the comparison between the scans and the FEM-Models the box with the strain gauges and the cables for the power supply and data exchange have to be deleted, because these areas are not included in the FEM-Model.

After the filtering these scans have to be transformed into the coordinate system of the FEM-Model. This step is realized with CloudCompare. For the transformation four points in the scan and the FEM-Model are chosen for a classical 3D-Helmert-Transformation. This transformation is calculated for the initial position. With the resulting transformation parameters the other position are transformed.

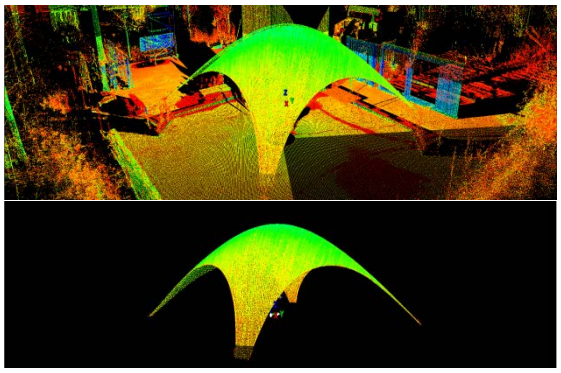

Fig 7 Point cloud before and after filtering

Further, the modelling of the 3D point clouds was performed with the software Geomagic Studio by Geomagic Inc. During the modelling process, a surface model S' that approximates the measured surface S was created from the point cloud assumed to lie on or near S.
The modelling program converted the given point cloud into a consistent polygonal model, called mesh. This operation generates the vertices, edges and facets that describe the surface. The point clouds were processed in several steps: first of all a triangle mesh was built based on the point cloud (Fig. 8) due to the history of Geomagic's development and for the 3D comparison. Then holes and spikes in the mesh are smoothed and in the end a NURBS surface was created (Fig. 9) (Geomagic Studio, 2012). The NURBS model is discretized according to curvature, without any stochastically model; only the resolution is adaptable. More information about NURBS are given e.g. in Piegl and Tiller (1997). The surface of the shell was modelled in the same way for each scan.

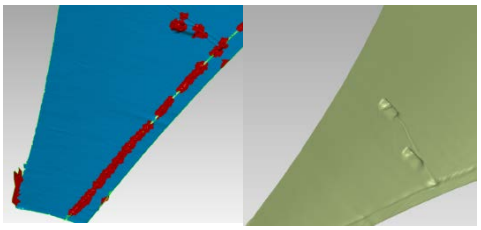

Fig 8 Point cloud to triangle mesh conversion

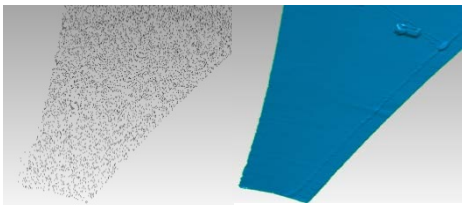

Fig 9 Triangle mesh auto-repair and creating NURBS surface

4 Deformation and FEM Analysis

The main purpose was to determine the deviations for each measuring epoch where the shape of the shell structure was changed and to recognize the areas where the deformations obtained with the laser scanner differ significantly relatively to the deformations recorded through the simulations.
For the deformation analysis the deviations between the compared models the shortest distance between the mesh points and the surface is calculated.

4.1 Deformation analysis of laser scans

For the deformation analysis, in order to compute and describe the deformations, two different epochs should be compared each time. The initial position of the shell structure, where no displacements have been applied, was used as the reference geometry to determine the deviations. This means that all the other scans were using this reference geometry to determine the deformations suffered by the structure.
Using Geomagic Qualify software, the deviations are computed as the shortest distances from the test surface to any point on the reference surface. These surfaces were modeled prior to the deformation analysis, as explained in chapter 3. The influence of the different supports displacements on the shell's position and shape can be clearly distinguished in the deformation results. In Fig. 10 the comparison between the laser scans of the initial position and the first displacement is shown. The left upper support, which will be called support 1 in the following, is moved 20 mm in X-direction for the first displace-

ment. The deformations can be easily observed as the comparison report is color-coded according to deformation values. The deformation results for the simulated data are obtained in the same way.

The Geomagic Qualify reports show color-coded images of the shell portraying the deformation values for each support displacement, as well as the points were the maximum positive and negative deviations are recorded. In the Fig.s 10, 11 and 12 the movements of the support 1 on the direction of the three axes, X, Y and Z are exemplified. In the same way has been proceeded for the other two supports. These results are similar and are not presented in this contribution.

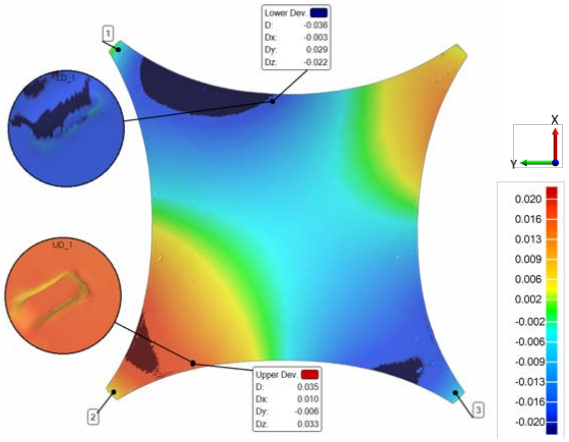

Fig 10 Color coded deformation of the movement from Support 1 in X axis direction

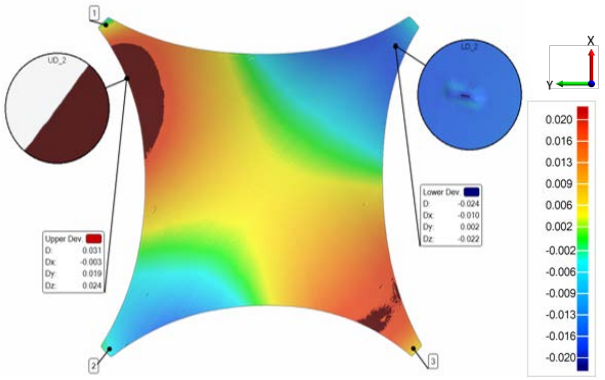

Fig 11 Support 1 moved in Y axis direction

For all three supports, the maximum upper and lower deviations were carefully analyzed, because these values could have been influenced by outliers. According to the deformation reports most of these values were found either on the sensor boxes, where the scanner could not record the data correctly due to an improper incidence angle, or at the edge of the shell surface, where the reflected signal was as well

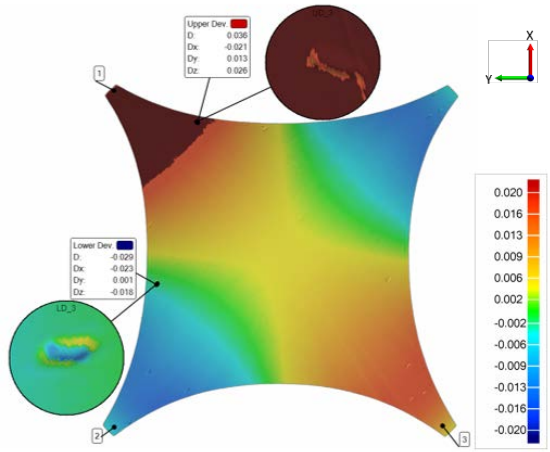

Fig 12 Support 1 moved in Z axis direction

affected by the incidence angle. Table 1 summarizes the results of the deformation analyses between the different support displacements situations and the initial situation. Pos. 1 to Pos 3 are the displacements on support 1. For each position the support was moved 20 mm. Pos. 1 was moved in X-direction, Pos. 2 in Y-direction and Pos. 3 in Z-direction. The results of the movements from support 2, which is the one on left bottom in the figures, are given in Pos. 4 to Pos. 6. Pos. 4 is the movement in X-direction, Y-direction is shown in Pos. 5 and the Z-direction is shown in Pos. 6. Pos. 7 to Pos. 9 are the movements of the third support. This is the support on the right bottom in the figures. Pos. 7 shows the movements in X-direction, Pos. 8 in Y-direction and Pos. 9 in Z-direction. The summarized results in Table 1 are the maximum and minimum deviations in each position, as well as the positive and negative average deviations. These values point out that the different epochs show comparable deviations caused by the hydraulic movements.

These deviations are investigated with a multiple statistical test for significant deformations. For the global test the test quantity is given by:

$$\chi^2 = \frac{\sum_{i=1}^{n} d_i^2}{2 \cdot n \cdot \sigma_{TLS}^2} \sim \chi_n^2 \qquad (1)$$

with d_i as deviation between the reference scan and the test scan, furthermore σ_{TLS} is the accuracy of the laser scanner coordinates, which is set to 1 mm and n is the number of deviations.

For the accuracy of the laser scanner a very simple model is used. Normally the standard deviation of the scanned coordinates depends on a lot of different factors like the instrumental errors. A detailed model is part of current research e.g. Kauker and Schwieger (2015) and Kauker and Schwieger (2016). Surprisingly, there are no significant deformations between the initial position and the moved positions according to the global test. An individual test is not necessary.

Table 1 Deformation analysis results for laser scanning

Position	Max. Up. Dev. [mm]	Min. Low. Dev. [mm]	Aver. Pos. Dev [mm]	Aver. Neg. Dev. [mm]
Pos. 1	35	-36	11	-11
Pos. 2	31	-24	10	-9
Pos. 3	36	-29	11	-8
Pos. 4	36	-33	10	-11
Pos. 5	27	-42	11	-12
Pos. 6	36	-37	12	-7
Pos. 7	33	-29	10	-9
Pos. 8	32	-40	10	-11
Pos. 9	37	-36	11	-8

These results are statistical correct, but non-realistic. One reason is that it is caused to the huge number n. It may be possible that the deviations are correlated, but the χ^2 test claim non-correlated parameters.

So alternatively, individual statistical tests are made, too. For these significance tests the Gaussian distribution was used, because the elementary error model is assumed, which is described in detail by Kauker and Schwieger (2015).

The test quantile y is defined as followed:

$$y = \frac{d}{\sqrt{2} \cdot \sigma_{TLS}}. \qquad (3)$$

In Table 3 the percentage of significant deviations for each epoch is given.

Table 3 Deformation analysis results for measurements

Position	Perc. of sign. dev. [%]
Pos. 1	87.1
Pos. 2	84.7
Pos. 3	84.6
Pos. 4	87.7
Pos. 5	85.9
Pos. 6	84.7
Pos. 7	85.6
Pos. 8	87.2
Pos. 9	84.8

4.2 Results of simulations

As example, the shell's deformations using the simulation data for support number 1 are shown in Fig.s 13-15, based on the Geomagic Qualify deformation analysis.

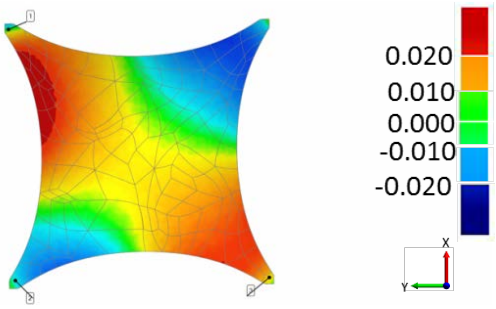

Fig 13 Simulation of support 1 moved in X axis direction

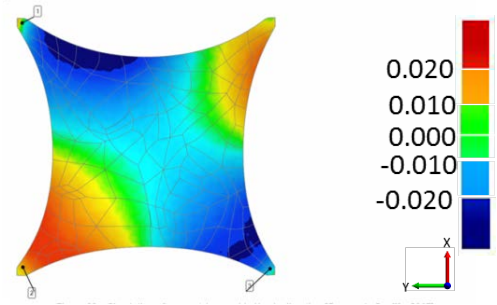

Fig 14 Simulation of support 1 moved in Y axis direction

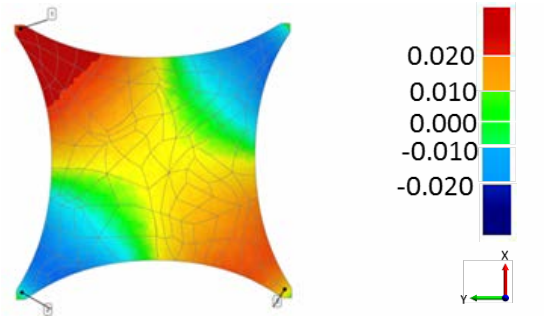

Fig 15 Simulation of support 1 moved in Z axis direction

The deformation analysis using simulation data has been performed for all three mobile supports of the Stuttgart SmartShell. The maximum upper and lower deviations, the average deviations and the standard deviations are listed in Table 4.

Table 4 Deformation analysis results for simulation model

Position	Max. Up. Dev. [mm]	Max. Low. Dev. [mm]	Aver. Pos. Dev. [mm]	Aver. Neg. Dev. [mm]
Pos. 1	20	-31	8	-10
Pos. 2	30	-20	10	-8
Pos. 3	28	-17	9	-7
Pos. 4	26	-30	8	-10
Pos. 5	21	-29	8	-10
Pos. 6	28	-16	9	-7
Pos. 7	30	-20	10	-8
Pos. 8	21	-30	8	-10
Pos. 9	28	-17	9	-7

4.3 Comparison of FEM – Model and laser scans

The most interesting part of this investigation is the comparison between the FEM-simulation and the laser scans, because the simulation shows the model state and the laser scans describe the actual measured.

As the analysis reports are color-coded according to deformation values, it can be easily noticed that even though the deformations detected with the laser scanning technology tend to be similar to the ones provided by simulations, some differences between the two methods exist. For example, in the bottom right corner of Fig. 16, there is a region exceeding deviation values of 20 mm that does not appear in the case of the simulation. At this stage of the research it is not absolutely clear if the deviations between planned and consequently simulated shape and realized shape of the SmartShell (Neuhäuser, 2014) or measurement errors are the reason for the difference.

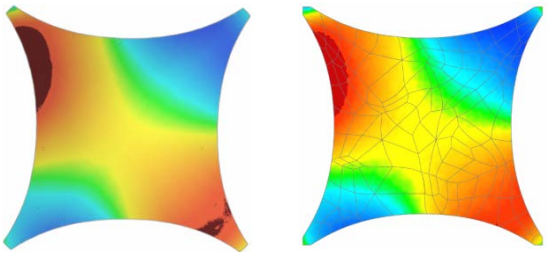

Fig 16 Comparison between laser scanning and simulation

For the comparison between the simulation results and the measurements a multiple statistical test is realized. For the global test the test quantity is given by:

$$\chi^2 = \frac{\sum_{i=1}^{n} d_i^2}{\left(\sigma_{TLS}^2+\sigma_{Reg}^2+\sigma_{Sim}^2\right)\cdot n} \sim \chi_n^2 \qquad (4)$$

with n as number of measured differences. Here the difference d_i is measured between the measured and the simulated result. The differences are Euclidian distances between the calculated points of on the surfaces. In this case the standard deviation for the simulations and the one for the registration have also been taken into consideration. The standard deviation of the simulations σ_{Sim} will be considered zero and the standard deviation of registration σ_{Reg} is set to 17 mm, given from the registration in CloudCompare. As described in 3.2, the registration is necessary because the laser scans are not in the same coordinate system as the simulations (laser scanner's coordinates system versus Stuttgart SmartShell's coordinates system). The high standard deviation can be explained by the fact, that the simulation describes the planned shape of the shell, but the built shell reflects the real geometry (Neuhäuser, 2014). The X^2 distribution is used with a confidence probability of 95 %. Like in the test in 4.1 all epochs show no significant deviations.

This result looks again non-realistic. Additionally clear systematic deviations are visible. Like in 4.1 the reasons for the not significant deviation could be correlations between the measurements.

The authors try a second approach and test individually for all positions by changing the probability level to 95 % as for the global test. The test is carried through like before, but the results are clearly

different, since the y=1.96 is valid now, and are presented in Table 5.

Table 5 Significant deviations between the simulation model and the laser scans

Pos.	Perc. of sign. dev. [%]
0	5.8
1	3.7
2	3.0
3	7.3
4	9.3
5	5.7
6	2.7
7	3.1
8	2.1
9	3.6

Fig. 17 shows the deviations between laser scan and simulation of the initial situation.

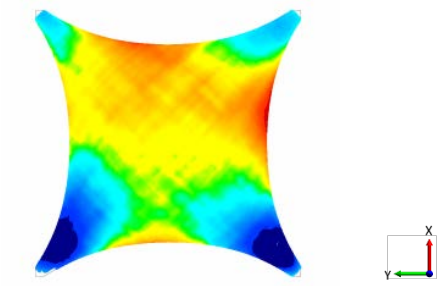

Fig 17 Deviations between laser scanning and simulation in initial situation

Two to nine percent of the deviations are significant although the significance level is estimated to 33 mm. This result looks more realistic, because the results of former investigations have shown deviations, too (Neuhäuser, 2014). Nevertheless if proper statistics are used, no significant individual deformations are detected. After construction of Stuttgart SmartShell in 2012, it was already scanned. The comparison between this laser scan and the simulation had shown similar results.

Another reason is that the simulations are designed for a material with homogeneous elastic modulus, in contrast wood is an inhomogeneous material and may change its behavior due to temperature, humidity and weather changes.

5 Conclusions

The investigations show that the given deformations of the Stuttgart SmartShell could be detected using terrestrial laser scanning. If the statistical correct way of multiple test is not followed. On the other side the terrestrial laser scanning measurement results show that some large deviations between the FEM model and the physical measured reality of the structure's movements are occurring. The percentage of significant differences between the deformations measured with the laser scanner and the ones determined based on the FEM model is between 2 – 9 % if the probability level is not chosen according to a multiple test. On the other side these percentage values are high if one considers that the significance level is 33 mm. If the mathematical correct way of multiple testing is followed no significant individual deformation could be detected. This on the one side contradicts the respective global test and on the other side is caused by the large uncertainty of the registration between FEM-model system and laser scanning system.

The registration error between scan and simulation for the initial epoch shows a high value of 17 mm, leading to the significance level of 33 mm.

A difference between planned model and the realized shell is assumed to be the main reason for the large differences but also for the bad standard deviation for the registration between FEM-model and scanner system. A new simulation using the really built geometry has to be realized in the future. The authors assume that the registration would deliver much smaller standard deviations thus leading to smaller deviations between the positions and to a lower significance level even in the multiple case.

Other reasons for these deviations may be scanner errors or influences of climate changes during the years.

Future work should also integrate all the influencing factors, like aging caused by weather and waterproofing and grinding, into the FEM model. In this way the behaviour of the shell may be modelled in a better way. Additional Stuttgart SmartShell should be scanned at least one a year to detect possible changes over the time.

References

Bathe, K. J. (2002). *Finite-Elemente-Methoden*. Springer, Berlin/Heidelberg

Eling, D. (2009) Terrestrisches Laserscanning für die Bauwerksüberwachung. PhD Thesis at the Gottfried Wilhelm Leibnitz University of Hannover. http://dgk.badw.de/fileadmin/docs/c-641.pdf..

Geomagic Studio (2012). *Product Specifications.* Available at: http://www.dirdim.com/pdfs/DDI_Geomagic_Studio_Wrap_2012.pdf [Accessed May, 2015].

Institut für Systemdynamik (2013). *Hybride intelligente Konstruktionselemente.* Available at: http://www.isys.uni-stuttgart.de/forschung/mechatronik/hike/ [Accessed May, 2015].

Kauker, S., Schwieger, V. (2015): *Approach for Synthetic Covariance Matrix for Terrestrial Laser Scanner*. In Proccedings for 2nd International Workshop on "Integration of Point- and Area-wise Geodetic Monitoring for Structures and Natural Objects"; March 23-24, 2015, Stuttgart, Germany.

Kauker, S., Schwieger, V. (2016): *First investigations for a synthetic covariance matrix for monitoring by terrestrial laser scanning*. 3rd Joint Symposium on Deformation Monitoring, Vienna, Austria, 30.03.-01.04.2016.

Neuhäuser, S., Weickgenannt, M., Witte, C., Haase, W., Sawodny, O., and Sobek, W. (2012): *Stuttgart SmartShell – A Full Scale Prototype of an Adaptive Shell Structure.* Journal of the International Association for Shell and Spatial Structures, vol. 54, no. 4, pp. 259-270.

Neuhäuser, S. (2014). *Untersuchung von Spannungsfeldern bei adaptiven Schalentragwerken mittels Auflagerverschiebung*. Ph.D. Thesis at Institute for Lightweight Structures and Conceptual Design, University of Stuttgart. http://elib.uni-stuttgart.de/opus/volltexte/2014/9278/pdf/Dissertation_Stefan_Neuhaeuser.pdf

Piegl, L., Tiller, W. (1997). *The NURBS book.* Springer, Berlin and New York.

Stuttgart SmartShell (2015). *Projekt.* Available at: http://smartshell-stuttgart.de/?page_id=19&lang=de [Accessed April, 2015].

Tsakiri, M.; Lichti, D.; Pfeifer, N. (2006). *Terrestrial laser scanning for deformation monitoring.* In Proceedings of the 12th FIG symposium on deformation measurements and 3rd IAG symposium on geodesy for geotechnical and structural engineering, Baden, Austria.

Zoog, H.-M., Ingensand H. (2008*). Terrestrial Laser Scanning for Deformation Monitoring – Load Tests on the Felsenau Viaduct (CH).* The Internatinal Archives of the Photogrammtry, Remote Sensing and Spatial Information Sciences. Vol. XXXXVII, Part B5, Beijing.